MATEC Web of Conferences **16**, 07005 (2014)
DOI: 10.1051/matecconf/20141607005

Identification of corrosion in reinforcement rebars by using the GPR

Z. Mechbal[1], A. Khamlichi[2]

[1]Communications Systems and Detection Laboratory; Abdelmalek Essaadi University, Tetouan 93002, Morocco
[2]Communications Systems and Detection Laboratory; Abdelmalek Essaadi University, Tetouan 93002, Morocco

Abstract. Considering the problem of corroded steel reinforcements buried in concrete members, a methodology based on ground penetrating radar was proposed for the identification of the corrosion affected zone. The method uses post-processing of radargram as obtained from a classic B-scan realized by the electromagnetic radar, when working with adequate high frequencies that are usually used for inspection of reinforced concrete structures. The radar displays are in general complex and not easy to interpret. However, significant information can be extracted from the obtained images to make a reliable report after the inspection. In this context, a correlation formula was proposed previously to estimate the perimeter of a reinforcement bar which is embedded in a concrete massif by using the radargram traces. This formula was employed in the present work in order to estimate the corroded zone perimeter. The obtained results have shown that it provides good prediction of the deterioration extent. Clear contrast of traces was noticed also while modifying the depth of the corrosion affected zone. However, to obtain the depth of the corroded segment of the rebar, further developments concerning image processing of a radargram are required.

1 Introduction

Ground Penetrating Radar (GPR) has been frequently used for the detection and mapping of subsurface utilities and other civil engineering infrastructures [1]. These electromagnetic radar systems are also widely used for the inspection of concrete structures in order to locate the reinforcements or to detect the presence of any damage [2]. GPR works on the principle of electromagnetic field propagation in a dielectric medium and on scattering of these waves by obstacles or discontinuities which generate reflected waves. These traces are processed to obtain a radargram either in the form of a B-scan or C-scan.

The outline profiles appearing in the B-scan [3] are generated by the propagation of short pulses into a medium with some electromagnetic properties. Most of the obtained pattern shapes in the GPR images take the form of hyperbolic curves or linear segments. The hyperbolic curves are generated by embedded objects having cross-section size of the order of the radar pulse wavelength; while the linear segments are due to planar interfaces existing between layers with different electrical characteristics.

Many tools have been developed to enable the interpretation of GPR data. The main objective is to determine the inverse problem solution in order to extract the information regarding the object causing a given observed hyperbolic curve for example. These include Hough transform [4] or neural network based algorithms as well as swift conic algorithms.

The recent advances in the special field of GPR used for diagnosis in reinforced concrete structures have enables to estimate both rebar position and cover depth with good accuracy, by performing adequate interpretation of the obtained radargram. Nowadays, steel reinforcements underlying in concrete structures can be detected and located with high accuracy by using appropriate procedures [1,5].

The common radars used in the field of concrete structures have the standard frequencies $f_1 = 1.5GHz$ or $f_2 = 2.6GHz$. These give a resolution of the order $40mm$ to $70mm$ which exceeds largely the habitual range of rebar diameter. Overestimation of diameters occurs then while trying direct exploitation of the radar scans. To correct these estimations, Chang et al. [6] proposed an empirical procedure for rebar diameter guess at the cost of operating advanced digital processing of the scans. They have illustrated the process on real applications realized for some concrete section geometry and reinforcement diameter. Other researches have also dealt with this problem by considering correlations rebar diameter and radar cross section [7].

The experimental evidence has shown that the accuracy of the previous approach has still to be enhanced. The authors have investigated the problem both experimentally and theoretically. They have used a finite-difference based code to model scattering from

concrete reinforcements. They have arrived at the necessity of collecting a radar profile with both E and H polarization which can be tackled by using a dual-polarized antenna [8]. Working with a frequency of $1GHz$, the highest sensitivity to rebar diameter occurred for diameters about 15 to $26mm$. While working with the case resolution was higher and optimal for diameters in the range $8–13mm$. The authors have pointed out that reproducibility of results is uncertain and concluded that a statistical analysis of the results should still be performed as in general a single measurement would be unreliable.

Alterations that could affect steel rebars such as corrosion can also be detected by using the GPR. High frequency antennas and pertinent post-processing of the echo signal are to be used in this last case. Different GPR signatures may be used for detecting internal corrosion of steel reinforcement within the concrete. Moisture and dissolved chlorides within the concrete attenuate the radar signals that are reflected from embedded rebars [9]. They also decrease the velocity of the wave signal and increase arrival times. Generally, lower reflection magnitude and greater travel time are indicative of larger corrosion or deterioration affecting the inspected rebar.

Analysis of rebar reflection features can be performed in order to extract information about the corrosion state and to determine the reflectivity of the corroded rebar. A threshold level was determined to differentiate between good and corroded rebars [10]. The authors have reported that the radar amplitude data of rebar reflection can be used to indicate whether the corrosion had occurred.

The location and cover depth of reinforcing steel in concrete structures has a great effect on the condition of that structure. A thin cover depth would result in rapid reinforcement corrosion, and therefore lead to early deterioration. Rebar corrosion can cause cracking of the concrete cover which lead to a decrease of load-carrying capacity of structural members. The threshold of reflection amplitude used to discriminate the good and corroded rebar can change from one project to another. It is influenced by many factors such as the water and chloride content of rebar cover and the type of the concrete in which the rebar is embedded. So there is a crucial need for further study before the GPR can be used in practice to operate detection of rebar corrosion.

The objective of this work is to assess detectability of localized corrosion defects by using the GPR. The aim is to investigate how the signatures that result from a reinforcing steel bar and a corrosion defect that it contains could be used to identify the extent of damage. As the degree of precision with which defects can be identified is a major concern, focus will be done on adequacy of the frequency with regards to target resolution and also on quantification of the defect size.

2 Modelling reflection traces of the GPR

2.1 Physical base of the GPR

The GPR operates by the emission of a sequence of very short electromagnetic pulses into the medium by using an adequate antenna. The centre frequency is usually between $100\,MHz$ and $2.6GHz$. If abrupt changes occur in the dielectric properties of the medium then part of the electromagnetic energy will be reflected back to the inspected surface. This can be recorded and amplified by the receiving antenna which may in many applications coincide with the emitting antenna. The recorded signal is registered as amplitude and polarity versus two-way travel time.

In air, the speed of propagation of an electromagnetic wave has the constant value $c=3\times10^{8}\,m.s^{-1}$. In a solid or liquid medium the velocity of electromagnetic waves is reduced. It is given as function of the relative dielectric permittivity, ε_r, the relative magnetic permeability, μ_r, and the electrical conductivity, σ, by

$$V=\frac{c}{\sqrt{\varepsilon_r\mu_r\frac{1+\sqrt{1+\eta^2}}{2}}} \tag{1}$$

with $\eta=\sigma/(\omega\varepsilon)$ the loss factor, where $\varepsilon=\varepsilon_r\varepsilon_0$ is the dielectric permittivity, $\varepsilon_0=8.854\times10^{12}\,F.m^{-1}$ the dielectric permittivity in free space and $\omega=2\pi f$ the angular frequency in which f represents the frequency.

In non-magnetic ($\mu_r=1$) low-loss materials where η 0, the velocity of electromagnetic waves simplifies to the expression

$$V=\frac{c}{\sqrt{\varepsilon_r}} \tag{2}$$

For resistive (low-loss) materials, equation (2) shows that the velocity of electromagnetic waves propagating in a solid medium is decreased in comparison with the velocity in air. The maximum decrease can reach the relative factor of nine, this is for instance the case of fresh water where the velocity of propagation is only of order $V_w=0.34\times10^{8}\,m.s^{-1}$.

Geometric and physical attenuation mechanisms lead to reduction of the electromagnetic signal strength during propagation in a particular medium. Localized losses such as those due to reflection/transmission at interfaces and scattering of energy can modify also significantly the signal. Scattering happens when an object has a dimension comparable to the wavelength and this phenomenon turns out to be further marked for high frequencies. The attenuation is function of dielectric permittivity, magnetic permeability and electrical conductivity as well as the work frequency. The attenuation coefficient is expressed as

$$\alpha=\omega\sqrt{\varepsilon\mu\frac{\sqrt{1+\eta^2}-1}{2}} \tag{3}$$

For low-loss materials, the attenuation coefficient simplifies to the following equation

$$\alpha=\frac{\sigma}{2}\sqrt{\frac{\mu}{\varepsilon}} \tag{4}$$

Equation (4) shows that attenuation is proportional to the electrical conductivity, so as high attenuation occurs in materials with high electrical conductivity.

One of the characteristics of the GPR is the penetration depth. This faculty is controlled by the GPR centre frequency, the electrical conductivity and the attenuation of the medium of propagation. In resistive materials that admit low-loss factor, a low centre frequency enables a large penetration depth whereas a high centre frequency yields a reduced penetration depth.

Another key characteristic of the GPR is the resolution power. The vertical resolution depends on the work wavelength, λ, of the propagating electromagnetic wave. This is determined by the GPR frequency and velocity of the material according to $\lambda=V/f$. For a given work frequency, the distance that can be discerned between two reflectors should be greater than $1/2$ the wave length λ [11]. One can then notice that the vertical resolution is increased while increasing the centre frequency.

As to the lateral resolution, it depends, in addition to the wavelength of the propagating electromagnetic wave, on the depth to the target as well as on the antenna mode of focusing used. In case of sedimentology ground problems, Neal [12] discussed in detail the different aspects that have to be taken into account in the evaluation of the lateral resolution.

For a spherical wave that can be used to schematize the radar problem, the radiated energy expands laterally as it propagates downwards, resulting in a decrease in this direction of the horizontal resolution. Energy transmission for a spherical wave is however quite different from that in radar as the GPR antenna is made from dipoles that generate polarised wave fields, with the consequence of strong directionality to amplitudes [13-14].

Radiated energy creates an electromagnetic field within 1.5 wavelengths of an antenna [13]. Therefore, the part of the inspected medium within this zone defines the near-field zone and constitutes part of the antenna [15]. Beyond this zone one finds the far-field zone in which energy can be transmitted.

2.2 Hyperbolic signature in GPR radargram

The hyperbolic signatures in GPR data are created by reflection that occurs on the target boundary with changing distance between the antenna and the target. Let's assume within the framework of two-dimensional approximation of the problem, as is the case of a B-scan, that the target is a circle of radius r and located at the point of coordinates (x_0,z_0+r) as shown if figure 1.

If the antenna is located at the point $(x,0)$, then the following geometrical relation will hold

$$(d+r)^2=(z_0+r)^2+(x-x_0)^2 \tag{5}$$

where d is the actual distance separating the antenna from the target surface. This distance is related to the two-way travel time or delay time of reflected signal by

$$d=\frac{Vt}{2} \tag{6}$$

where V is the signal velocity in the medium as given by equation (2).

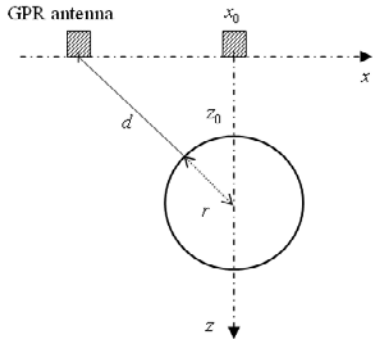

Fig. 1. A buried cylindrical object in a B-scan configuration.

Denoting t_0 the delay time corresponding to antenna in the position x_0, one obtains the relation between the two-way travel time t, the horizontal position x and the velocity of propagation V as

$$\left(\frac{t+2r/V}{t_0+2r/V}\right)^2-\left(\frac{x-x_0}{r+Vt_0/2}\right)^2=1 \tag{7}$$

When there is only a single point, then $r=0$. For a target which is not a circle, but which has a round pattern which is close to it, the ray $r(t)$ will be function of time.

By letting $a=t_0+2r/V$, $b=r+Vt_0/2$, $y=t$ and $y_0=-2r/V$, equation (7) can be related to that of a general hyperbola as

$$\frac{(y-y_0)^2}{a^2}-\frac{(x-x_0)^2}{b^2}=1 \tag{8}$$

If t_0 and the parameters related to the hyperbola (a,b) are identified from the radargram, the velocity, depth and the radius can be estimated by the following equations

$$V=\frac{2b}{a},\ z_0=b\frac{t_0}{a} \text{ and } r=b-\frac{bt_0}{a} \tag{9}$$

Giving a radargram, curve fitting techniques can be used to identify the parameters a and b. From the minimum two-way time t_0, one can then get the characteristics of the rebar. However, from a practical point of view, when r is small as is the general case of rebars used in concrete reinforcement, the expression

giving r in equation (9) is very sensitive to errors that influence the determination of the three parameters a, b, t_0 and the results are inaccurate. This is why other direct methods were introduced [6].

2.3 Practical method for identifying rebars section

The GPR based inspection of reinforced concrete structures deals with the main problem of identifying the size, shape, depth, and location of the buried rebar. A B-scan constitutes the most evident method to achieve this task by analyzing the GPR reflected images. Data provided by these images consist of amplitude traces of reflected wave. Each of these reflection traces contains a series of waves that vary in amplitude depending on the amount and intensity of energy reflection that occurs at the buried rebar interfaces. One should notice however that because of real GPR units operation the reflected signal comes from conical beams which can then be recorded even though the antennas are not directly over the reflecting rebar. The radar detects rebar from a number of different angles with variable distances separating them.

A formula for estimating the approximate size of the radar footprint, figure 2, that is to say the area illuminated on a buried surface, and which is based on subsurface permittivity, radar work wavelength and depth to a horizontal reflector, is given by Chang et al. [6]

$$A=\frac{\lambda}{4}+\frac{z_0}{\sqrt{\varepsilon_r+1}} \tag{10}$$

where A is the approximate long dimension radius of the footprint and ε_r the equivalent relative dielectric permittivity to depth z_0 of the reflector surface.

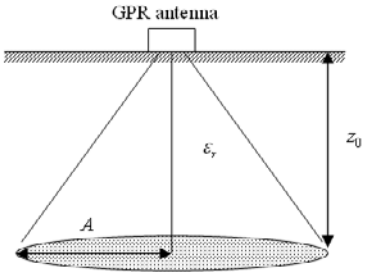

Fig. 2. The GPR footprint in the medium, all part outside this area will have no significant reflection.

When a propagating electromagnetic wave encounters a subsurface discontinuity with respect to one of the parameters ε_r, μ_r or σ, some energy is reflected. Reflection strength is proportional to the magnitude of change [16]. The amount of energy reflected, with respect to signal amplitude, is given by the reflection coefficient R. Assuming that σ and μ_r contrasts are negligible; the reflection coefficient is given by

$$R=\frac{\sqrt{\varepsilon_{r,2}}-\sqrt{\varepsilon_{r,1}}}{\sqrt{\varepsilon_{r,2}}+\sqrt{\varepsilon_{r,1}}} \tag{11}$$

where ε_r^1 and ε_r^2 are the relative permittivity of the adjacent layers 1 and 2.

The value of R lies in the interval $[-1,1]$. In order to measure a significant reflection, the coefficient of power reflectivity is employed. This coefficient is defined as

$$P_r=R^2 \tag{12}$$

Considering a configuration of reinforced concrete as that one depicted in figure 3, a B-scan consists in moving at constant speed the antenna along a line. The electromagnetic waves are transmitted through an antenna to the concrete. Since the concrete material is assumed to be homogeneous, the dielectric constants of the concrete and the rebar are constant. When the antenna is right on the vertical passing through the centre of the rebar, the reflection signal as function of time will show variable amplitude. This is due to the internal interfaces showing a contrast in the dielectric properties.

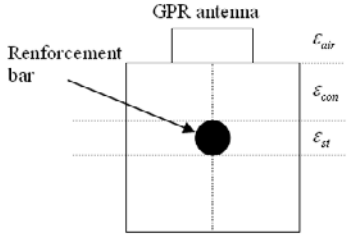

Fig. 3. Configuration of a rebar buried in concrete and the contrast permittivity causing reflection.

Recording the reflected pulses from these interfaces enable to estimate the dielectric constants: ε_{air}, ε_{con} and ε_{st}. This can be performed readily from the recorded signal amplitudes at each interface, by using equations (4) to (7) as given in reference [6].

The coefficient of power reflectivity, composing the GPR radargram, takes into account all reflections occurring in the medium: from the first reflection happening when the obstacle enters the energy zone, shown in figure 2, to the last reflection which corresponds to the obstacle leaving that zone.

Denoting L the measured length of the contrast zone on the radargram, which starts from the initial point of power reflectivity to the final point, one can use the following relation to estimate the geometric length of the round obstacle [6]

$$L_{obs}=L-2A \tag{13}$$

In case of rebars, the length of the obstacle coincides with the perimeter of the rebar $L_{obs}=2\pi r$, equations (2), (9), (10) and (13) yield then the rebar radius as

$$r=\frac{L}{2\pi}-\frac{V}{4f\pi}-\frac{ct_0V}{2\pi\sqrt{c^2+V^2}} \quad (14)$$

3 Results and discussion

The modelling was performed by using Reflexw software package [17]. Concrete specimens containing a buried reinforcement bar with various corroded zone depths were modelled. The corrosion defect dimensions corresponded to a length ℓ=81mm and depth equal to h=3mm or h=6mm. Figure 4 presents the concrete section modelled under Reflexw, it has a square geometric form with the edge dimension equal to 400mm.

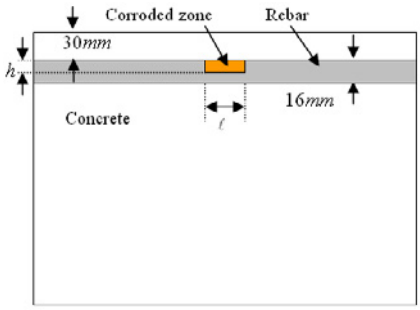

Fig. 4. Configuration of the corroded rebar and parameters of the corrosion affected zone.

Figure 5 presents the model developed under the CAE interface of Reflexw for ℓ=81mm and h=6mm.

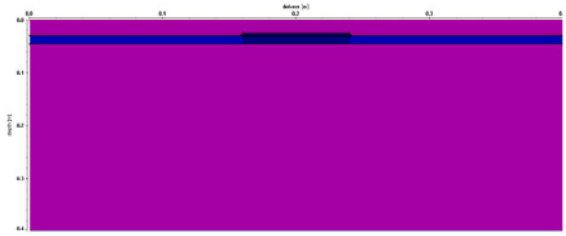

Fig. 5. Geometry of the model developed under Reflexw for ℓ= 81mm and h= 6mm.

The dielectric properties used for the different materials are given in table 1.

Table 1. Materials properties used during simulations.

Material	Permittivity ε_r	Permeability μ_r	Conductivity σ
Concrete	6	1	0.0255
Steel	1.45	10^4	9.931×10^6
Air and corrosion	1	1	0

The simulation parameters under Reflexw were selected as follows:
- the wave form excitation was of Kuepper mode;
- the source type was selected to be exploding reflection;
- the boundary conditions were chosen to be linear absorbing range;
- the output type was single line which corresponds to B-scan;
- the trace number was fixed at 12 ;
- the time window was fixed at $0.3\times10^{-9}s$;
- and the summation width at 50 .

Table 2 gives the other simulation constants as function of the chosen antenna.

Table 2. Materials properties used during simulations.

	Antenna 1.5GHz	Antenna 2.6GHz
Central frequency MHz	1500	2600
Time window s	12×10^{-9}	8×10^{-9}

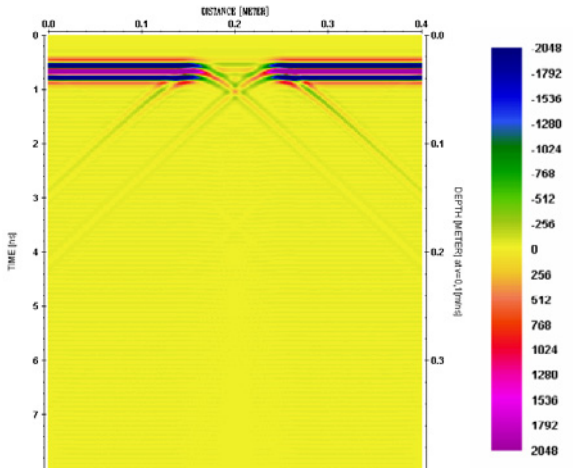

Fig. 6. Radargram for the case h=3 mm and f_1=1.5GHz .

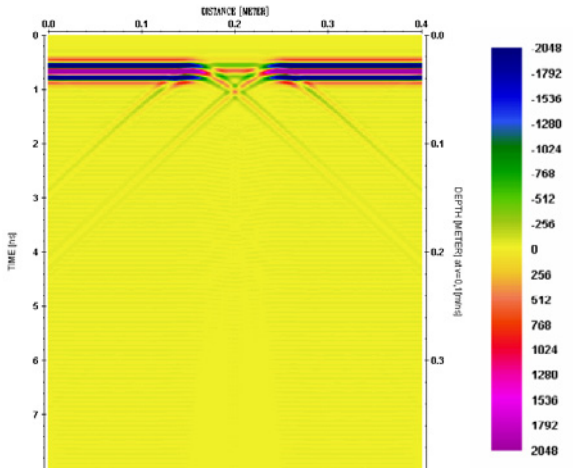

Fig. 7. Radargram for the case h=3 mm and f_2=2.6GHz .

The obtained scans for the four cases are shown in figures 6 to 9 as function of the corrosion depth h and the work frequency: 1.5GHz or 2.6GHz .

One can see that the corrosion defect trace is visible on all the radargrams and that the contrast is better for the work frequency $f=2.6\,GHz$.

Using the post-processing tools, one can identify the hyperbola parameters and then obtain the velocity of electromagnetic waves in concrete which is here $V=1.23\times10^{8}\,m.s^{-1}$. The two-way time can be estimated from the radargram, the obtained value is here $t_0=2.5\times10^{-10}\,s$. One finds then by using equation (10) the following values of footprint radius: $A_1=0.0343$ for the work frequency $f_1=1.5GHz$ and $A_2=0.0257$ for the work frequency $f_2=2.6GHz$.

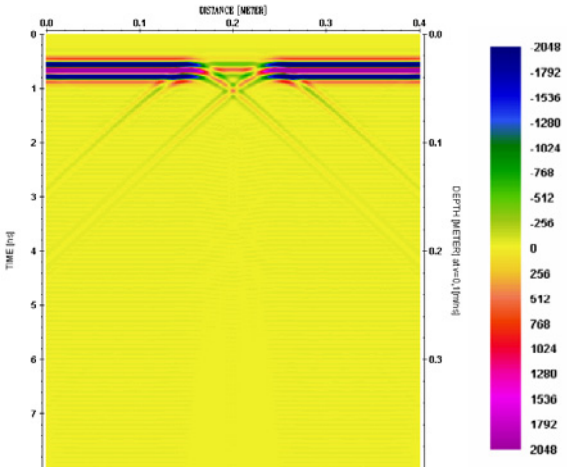

Fig. 8. Radargram for the case $h=6\ mm$ and $f_1=1.5GHz$.

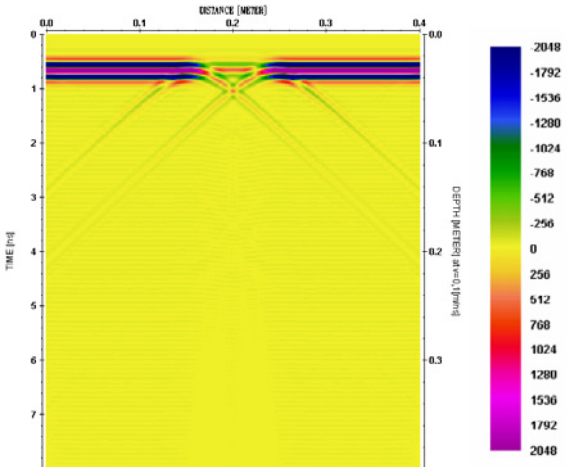

Fig. 9. Radargram for the case $h=6\ mm$ and $f_2=2.6GHz$.

From the radargram one obtain $L_1=0.17m$ and $L_2=0.14m$. By using now equation (13), estimation of the perimeter of the corroded zone can be performed. The obtained results are: $L_{obs,1}=L_1-2A_1=0.101m$ and $L_{obs,2}=L_2-2A_2=0.0886m$. These results are not far from the exact perimeter of the corroded zone of the rebar which is $0.093m$. To obtain the corrosion depth, image processing is needed. One can see that figures 6 and 8 on one hand and figure 7 and 9 on the other hand present a clear contrast, as the traces are more pronounced for the depth $h=6mm$ than for $h=3mm$.

4 Conclusions

Identification of the perimeter of a corroded segment of a rebar buried in concrete was considered in this work. The proposed methodology is based on post-processing of radargram as obtained from classic B-scan realized by the GPR, when working with high frequencies that are commonly used for inspection of reinforced concrete structures. A correlation formula used previously to estimate the perimeter of reinforcement bars was applied here and the obtained results have shown that its capacity to predict with good accuracy the perimeter of the corroded zone. Further developments concerning image processing of radargram are required to correlate the traces contrast with the depth of the corroded zone.

References

1. A. Dell'Acqua, A. Sarti, S. Tubaro, L. Zanzi, Signal Processing, **84**, 4 (2004)
2. J. Hugenschmidt, A. Kalogeropoulos, F. Soldovieri, G. Prisco, NDT&E Int, **43** (2010)
3. C. Bruschini, B. Gros, F. Guerne, P. Y. Pièce, O. Carmona, Journal of Applied Geophysics, **40**, 1-3 (1998).
4. J. Illingworth, J. Kittler, Computer vision, graphics, and image processing, **44**, 1 (1988)
5. M.R. Shaw, S.G. Millard, T.C.K. Molineaux, M.J. Taylor, J.H. Bungey, NDT&E Int, **38** (2005).
6. C.W. Chang, C.H. Lin, H.S. Lien, GPR. Constr Build Mater, **23** (2009)
7. V. Utsi, E. Utsi, *Proceedings of the tenth international conference on ground penetrating* radar (Delft, 2004)
8. M. Lualdi, L. Zanzi, M. Ciano, *Proceedings of the 11th international conference on GPR* (Columbus Ohio, 2006)
9. C.L. Barnes, J.F. Trottier, D. Forgeron, NDT & E International, **41**, 6 (2008)
10. S.S. Hubbard, J. Zhang, P.J.M. Monteiro, J.E. Petrson, Y. Rubin, ACI Mater. J., **100**, 6 (2003)
11. I. Møller, H. Vosgerau, Near Surface Geophysics, **4** (2006)
12. A. Neal, Earth-Science Reviews **66** (2004)
13. N. Engheta, C.H. Papas, C. Elachi, Radio Sci., **17** (1982)
14. R.L. Roberts, J.J. Daniels, J. Environ. Eng. Geophys., **1** (1996)
15. L.B. Conyers, D. Goodman, *Ground-Penetrating Radar: An Introduction for Archaeologists*. (Altamira Press, 1997)
16. J.M. Reynolds, *An Introduction to Applied and Environmental Geophysics*. (Wiley,1997)
17. K.J. Sandmeier, *Reflexw version 6.0*, (Karlsruhe, 1998)